ORIGINAL CONTRIBUTION

Optimization of Fluoroscopic MR Imaging Sequences on a Clinical 1.5T Closed Magnet System : Comparison between Single-shot Turbo Spin Echo and Turbo Field Echo Sequences

Hatsuho MAMATA[1], Taizou KOMIYA[2], Isao MURO[2], Seiya MATSUYAMA[1]

[1]*Department of Radiology, Tokai University School of Medicine*
[2]*Tokai University Hospital, Clinical Radiology Center*
Bohseidai, Isehara-shi, Kanagawa 259–1193

(Purpose) To evaluate the potential fluoroscopic capability of the sequences available on a clinical 1.5T closed magnet system.

(Materials and methods) For fluoroscopic imaging sequences, we chose a single-shot spin echo (SS-TSE) sequence with area selective imaging capability. T_1 and T_2-weighted turbo field echo (TFE) sequences were also evaluated as alternative imaging methods. We performed imaging of phantoms and normal brains to evaluate signal to noise ratio (SNR) and contrast to noise ratio (CNR) with SS-TSE and TFE sequences. For the evaluation, different temporal resolution, matrix sizes and FOVs were applied. We also evaluated the width of biopsy needle and foldover artifacts in each sequence.

(Results) In SS-TSE, SNR and CNR were improved as the temporal resolution attenuated from 0.3 to 1.0 s/shot. T_1-weighted TFE revealed excellent CNR with the temporal resolution of 0.3 and 0.5 s/shot when the matrix sizes were relatively small ($52–96 \times 128$). SS-TSE was less susceptible to metal artifact than TFE sequences. Area selective imaging capability of SS-TSE was convenient to obtain better temporal resolution without suffering from foldover artifacts.

(Conclusion) SS-TSE and T_1-weighted TFE sequences are feasible, when they are well optimized, for fluoroscopic monitoring of MR-guided procedures on a clinical 1.5T closed magnet system.

INTRODUCTION

In recent years, the development of open type magnet system made MR-guided procedures more feasible as minimally invasive methods[1)~4)]. Even with a closed system, if the magnet and its enclosure are designed to allow the operators to access the patients without

Keywords MR fluoroscopy, interventional MR imaging

particular obstacles, it may provide the same opportunity to perform these procedures[5),6)]. In that occasion, what becomes the real issue is the availability of imaging sequence optimized for fluoroscopic monitoring[7)]. Fast gradient echo type fluoroscopic sequence is commonly used for MR-guided procedures in an open magnet system, because it is more susceptible to MRI compatible needles so that the needle can be visualized accurately during the procedure. Where the larger magnetic field is available, this susceptibility artifact of the needle will become more apparent[8)~10)]. This means, vice versa, accuracy of the needle tip localization becomes less accurate in the larger magnetic field system. Moreover, spin echo sequence can provide better visualization of the needle in that occasion. The single-shot turbo spin echo sequence that we applied in this study can provide area-selective imaging capability also. The purpose of this study is to evaluate the potential fluoroscopic capability of the sequences available on a clinical 1.5T system with a closed magnet.

MATERIALS AND METHODS

1. Fluoroscopic imaging sequences

For fluoroscopic imaging, we chose a single-shot turbo spin echo sequence (SS-TSE) with area-selective imaging capability. T_1-weighted and T_2-weighted turbo field echo (TFE) sequences were also evaluated as alternative imaging methods. All studies were performed on a 1.5T superconducting unit of closed magnet system (ACS-NT, Philips, Netherlands).

For imaging, we employed two rectangular FOVs : 25 and 45 cm, respectively, with 40% reduction of phase encoding views for SS-TSE sequence, and 20% reduction for TFE sequences which was designed to eliminate fold-over artifacts. Matrix sizes varied from 86×128 to 56–256×256 in SS-TSE and 52×128 to 167×256 in TFE.

First, a phantom was imaged by SS-TSE sequence with different temporal resolutions by changing the scan times from 0.3 to 1.0 s/shot with an incremental step of 0.1 s. Other imaging parameters were fixed as follows : a 5 mm thick slice ; TE=126 ms ; echo train length=43 or 51 and a total of 30 shots which allowed 3 s fluoroscopic imaging with 0.3 s/shot temporal resolution, and 30 s fluoroscopic imaging with 1.0 s/shot. Image reconstruction time was 0.01 s and time delay for monitor display was 0.01 s. Then the images by T_1 and T_2-weighted TFE sequences were obtained with variable matrix sizes as indicated in Table 1 with following parameters : a 5 mm thick slice ; TR/TE/FA=8/3/20 for T_1-weighted TFE and 7.2/2.8/20 for T_2-weighted TFE.

2. Phantoms

To evaluate their potential feasibility for fluoroscopic imaging, we performed a phantom study using two pan-shaped coagulated vegetable oil phantoms containing hard-boiled eggs inside, one with 20 cm in diameter and 10 cm in height, and the other with 10 cm in diameter and 5 cm in height. Following puncture of the phantom by a 22 gauge MR compatible biopsy needle (0.8 mm in width) with its insertion angle 75 degrees to the static magnetic field, it was imaged by SS-TSE, T_1 and T_2-weighted TFE fluoroscopic imaging sequences, respec-

Received Nov. 18, 1998 ; revised Dec. 21, 1998
Reprint requests to Hatsuho Mamata, Department of Radiology, Tokai University School of Medicine, Bohseidai, Isehara-shi, Kanagawa 259–1193

tively.

3. Evaluation of signal to noise ratio (SNR)

We calculated SNR from phantom images obtained by each sequence. ROIs were selected on the image of the phantom itself and on the background. SNR was given by the phantom signal divided by the background signal. Number of pixels in a ROI was 832. In SS-TSE images, SNRs were calculated with different temporal resolutions, which were applied by changing TR with incremental steps of 0.1 s. SNRs in TFE sequences were calculated with different temporal resolutions, which were applied by changing matrix sizes. TR did not change as temporal resolution altered. In addition, SNR with different FOVs (25 and 45 cm) were calculated in each sequence. A birdcage head coil was used with 25 cm FOV and a body coil was used with 45 cm FOV. SNR was calculated three times and averaged.

4. Evaluation of contrast to noise ratio (CNR)

For evaluation of CNR, brain images of two normal volunteers were taken with SS-TSE, T_1 and T_2-weighted TFE sequences with temporal resolution of 0.3, 0.5, 0.8 and 1.0 s/shot. Matrix sizes varied from 52×128 to 256×256. ROIs were selected on the cortex, the deep white matter and the background. CNR was given by the signal difference between the cortex and the white matter divided by the background signal. The signal difference between the cortex and the deep white matter was given by the absolute value. Number of pixels in a ROI was 363. CNR was calculated three times and averaged.

5. Susceptibility and foldover artifact

Susceptibility artifacts were evaluated by measuring the width of the MR compatible needle demonstrated on the phantom image taken by each sequence. The needle width was originally 0.8 mm (22 gauge) and its insertion angle to the static magnetic field was 75 degrees. The imaging was performed with the temporal resolution of 1.0 s/shot, 25 cm rectangular FOV with 40% reduction of phase encoding view using a 10 cm diameter phantom in the birdcage head coil.

We used the larger phantom (20 cm diameter) in a birdcage head coil to evaluate foldover artifact with the temporal resolution of 1.0 s/shot, 25 cm rectangular FOV with 50% reduction of phase encoding view in each sequence.

RESULTS

1. Evaluation of SNR

In SS-TSE sequence, SNR with a matrix size of 128×256 became improved as the temporal resolution attenuated from 0.5 to 1.0 s/shot (Table 1), indicating SNR improvement along TR elongation. Even with the temporal resolu-

Table 1. SNR with Different Temporal Resolution

s/shot	0.3	0.4	0.5	0.6	0.7	0.8	0.9	1.0
SS-TSE	43.4 (56×256)	72.8 (59×256)	36.0 (128×256)	65.7 (128×256)	74.5 (128×256)	79.7 (128×256)	85.8 (128×256)	94.0 (128×256)
T_1-TFE	46.6 (52×128)	—	33.5 (96×128)	—	—	21.4 (128×256)	—	18.5 (167×256)
T_2-TFE	49.9 (52×128)	—	32.6 (96×128)	—	—	19.5 (128×256)	—	16.6 (167×256)

( ) : matrix size

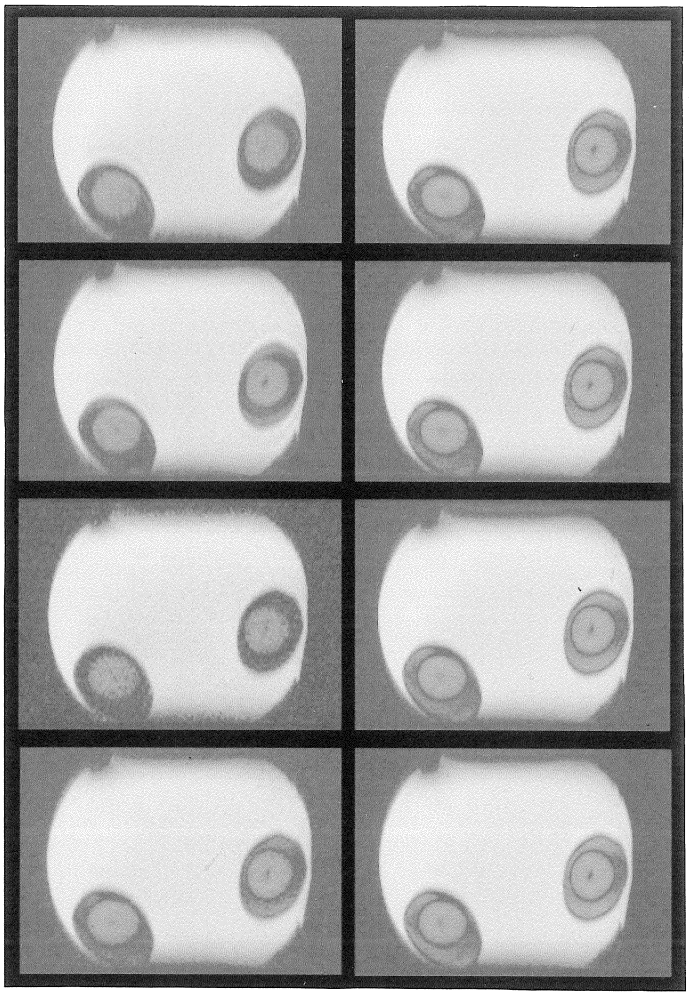

Fig. 1. SS-TSE with different temporal resolution. a : image with 0.3 s/shot temporal resolution. b : 0.4, c : 0.5, d : 0.6, e : 0.7, f : 0.8, g : 0.9, h : 1.0 s/shot. SNR improves as the temporal resolution attenuates from 0.3 to 1.0 s/shot. Note the obvious blurring of egg's contour at 0.3 (a) and 0.4 s/shot (b) where the matrix sizes are relatively small.

tion limited to 0.3 or 0.4 s/shot, SNR of the images with a smaller matrix size (56–59 × 256) were better than that with a larger one (128 × 256), though blurring of the needle edge and egg's contour had occurred (Fig. 1).

In TFE sequences, SNR became worse as the temporal resolution lowered, because of the increase of the matrix size (Table 1). Never-

Table 2. SNR with Different FOVs and Coils

coil (FOV)	Head (25 cm)	Body (45 cm)
SS-TSE (256 × 256)	120.6	77.3
T_1-TFE (167 × 256)	43.4	15.4
T_2-TFE (167 × 256)	33.9	13.6

All images were taken with the temporal resolution of 1.0 s/shot

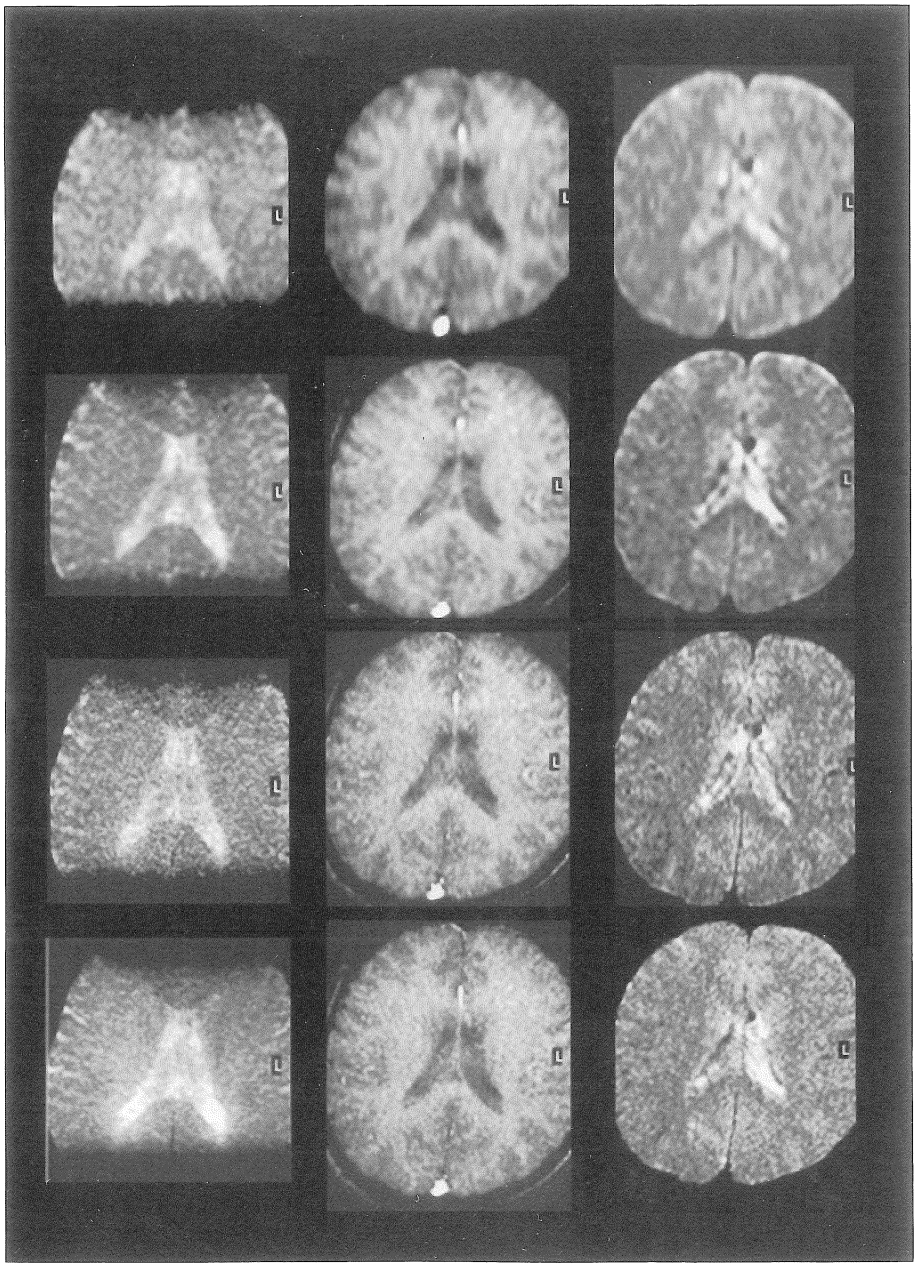

a	e	i
b	f	j
c	g	k
d	h	l

Fig. 2. Normal brain images in SS-TSE (a-d), T_1-weighted TFE (e-h) and T_2-weighted TFE (i-l) with different temporal resolution. Temporal resolution of the images : top to bottom, 0.3 (a, e, i), 0.5 (b, f, j), 0.8 (c, g, k), 1.0 (d, h, l)s/shot. In SS-TSE, CNR improves as the temporal resolution attenuates from 0.3 to 1.0 s/shot. Note relatively better tissue contrast in T_1-weighted TFE images (e-h).

Table 3. CNR with Different Temporal Resolution

s/shot	0.3	0.5	0.8	1.0
SS-TSE	0.9(86×128)	1.8(128×128)	1.6(256×256)	2.0(256×256)
T_1-TFE	6.4(52×128)	5.6 (96×128)	0.2(128×256)	0.4(167×256)
T_2-TFE	0.2(52×128)	0.4 (96×128)	0.7(128×256)	0.5(167×256)

( ) : matrix size

theless, blurring of the needle and egg's contour was less indicated on the images of the higher temporal resolutions of 0.8 or 1.0 s/shot.

The 25 cm FOV using a birdcage head coil offered much better SNR on the images taken with the temporal resolution of 1.0 s/shot than that of the 45 cm using a body coil in all sequences (Table 2).

2. Evaluation of CNR

In SS-TSE, CNR improved as the temporal resolution attenuated from 0.3 to 1.0 s/shot, although matrix size increased from 86×128 to 256×256 (Table 3).

In T_1-weighted TFE, with the temporal resolution of 0.3 and 0.5 s/shot, CNR was far superior to the other two sequences (Table 3, Fig. 2). With the temporal resolution of 0.8 and 1.0 s/shot, calculated CNR indicated the value down to a decimal point and it did not worth for evaluation.

T_2-weighted TFE images offered very poor SNR so that CNR with all temporal resolution became too noisy to evaluate.

3. Susceptibility and foldover artifact

The width of the biopsy needle measured on the image was : 4 mm on SS-TSE ; 8.7 mm on T_1-weighted TFE ; 8.2 mm on T_2-weighted TFE in contrast to the actual width of 0.8 mm, showing much reduced susceptibility artifact in SS-TSE (Fig. 3).

The images of 20 cm diameter phantom taken with rectangular FOV with 50% reduction of phase encoding view suffered from foldover artifacts in both TFE sequences, but not in SS-TSE sequence with area-selective imaging capability (Fig. 4).

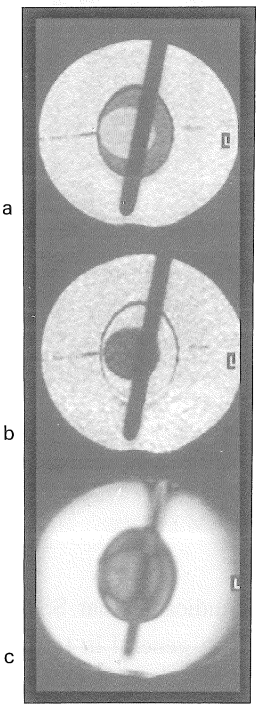

Fig. 3. Width of biopsy needles on the images. SS-TSE (c) showed the least susceptibility : 4 mm. T_1-weighted TFE (a) : 8.7 mm. T_2-weighted TFE (b) : 8.2 mm.

DISCUSSION

1. SNR

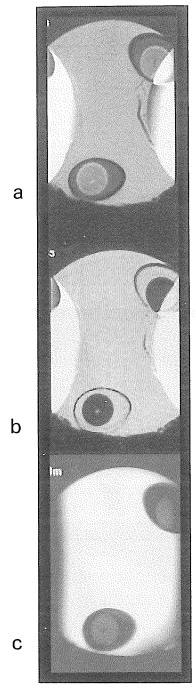

Fig. 4. Foldover artifact. a : T_1-weighted TFE, b : T_2-weighted TFE, c : SS-TSE. SS-TSE with area selective imaging capability is free from this artifact even with 50% reduction of phase encoding view.

Our results indicated that SS-TSE was superior to TFE in general in terms of offering excellent SNR, allowing us to access small lesions more precisely. In SS-TSE, there was a trade-off between increasing SNR and obtaining better temporal resolution. The more attenuated temporal resolution, the more increase in SNR. Further more, reducing phase encoding view of rectangular FOV had an advantage in obtaining better temporal resolution but it lowered SNR as the sequences with shorter scan time did. Increase of matrix size did not seem to affect SNR much in SS-TSE in present study, and even it made less blurred the object's contour.

In TFE sequences, we applied different temporal resolutions by varying matrix sizes, so that the larger matrix size was applied, the lower the temporal resolution was obtained. The SNR lowered as the temporal resolution attenuated. If matrix size were fixed to a certain adequate size and the temporal resolution were dependent on TR, SNR in these sequences would possibly to be improved better than that of this study. Furthermore, application of rectangular FOV with reduction of phase encoding view has capability to improve the temporal resolution. But reduction of phase encoding view will also lower SNR, and without area selective imaging capability like SS-TSE presented here, the images will suffer from foldover artifacts and they will be lethal for fluoroscopic imaging.

A 25 cm FOV using a birdcage head coil offered much better SNR than a 45 cm one using a body coil. There should be somewhat sensitivity difference between the head coil and the body coil, and this could affect the result. Application of a body array coil would be able to solve this sensitivity problem to obtain better SNR with body imaging. When matrix size is fixed, a smaller FOV will offer better spatial resolution. In present study, needle edge or egg's contour was less blurred on the images with a 25 cm FOV than a 45 cm one.

2. CNR

In SS-TSE, CNR improved as the temporal resolution attenuated from 0.5 to 1.0 s/shot as well as SNR. At the temporal resolution of 0.3 s/shot, the image became too noisy.

T_1-weighted TFE sequence offered excellent CNRs with 0.3 and 0.5 s/shot temporal resolution, far superior to the other two sequences. Obtaining good tissue contrast is an advantage to perform MR-guided biopsy of tumors and other lesions. With the temporal resolution of

0.8 and 1.0 s/shot, attenuated SNR due to the increase of matrix size made CNR low.

In terms of comparison between CNRs of SS-TSE and T_1-weighted TFE, the latter could offer better CNR with smaller matrix size and the former could offer better CNR with larger matrix size. Focussing on the temporal resolution of 0.5 s/shot where the applied matrix size was medium (128×128 in SS-TSE, 96×128 in T_1-weighted TFE), T_1-weighted TFE obtained better CNR than that of SS-TSE. Moreover, because of T_1-weighted nature of the sequence, the best tissue contrast will be offered particularly when used in combination with contrast agent administration.

In T_2-weighted TFE sequence, the images were too noisy to evaluate.

3. Susceptibility and foldover artifact

SS-TSE images less suffered from susceptibility artifacts compared with TFE sequences, which we agree with previous reports[8)~11)], to the extent that the needle tip could be positioned less erroneously. Though it is still thick enough to visualize on the images during MR guided procedures. In addition, the sequence is free from foldover artifacts because of its area selective imaging capability, even with a smaller rectangular FOV where the phase encoding view is reduced by 40 to 50%. Thus, the temporal resolution could be improved without foldover artifacts.

4. Future use of the fluoroscopic sequences in clinical cases

Well-optimized fluoroscopic sequences, especially SS-TSE and T_1-weighted TFE, will be the potential imaging methods for MR-guided procedures. They will be used for biopsy or minimally invasive therapy, e.g. cryotherapy, laser therapy and so on. When the procedure is performed, some kind of trick will be necessary. For example, liver moves by the diaphragmatic motion, so it needs to be stopped by holding breath when a puncture actually goes through. Letting patient breathe normally and telling him to hold his breath when the lesion appears best visualized on the monitoring system will make the procedure easier to perform. However, this MRI fluoroscopy will not be feasible for the organ that cannot be stopped its motion on purpose, like the heart. Because the temporal resolution of MRI fluoroscopy is not good enough to catch up with relatively fast movement, new design of faster sequence will be necessary for true real time fluoroscopic monitoring for moving object in the future.

CONCLUSION

What is crucial for the pulse sequences used for fluoroscopic monitoring in MR-guided procedures is the near real time imaging capability to delineate the target lesions with optimal CNR and SNR. In this study, we employed SS-TSE and TFE sequences as the potential imaging methods for the above purpose. As indicated by our results, the former was superior to the latter in terms of offering excellent SNR and CNR with good temporal resolution, less susceptible to metal artifacts and free from foldover, allowing us to access small lesions more precisely. In SS-TSE sequence, the most optimized fluoroscopic imaging can be obtained with following parameters : TR = 700 ms (which provides the temporal resolution of 0.7 s), a rectangular 25 cm FOV with 40–50% reduction of phase encoding view and a matrix size of 128×256.

In conclusion, SS-TSE and T_1-weighted TFE sequences are feasible, when they are well optimized, for fluoroscopic monitoring of MR-

guided procedures on a clinical 1.5T system with a magnet of a closed type.

ACKNOWLEDGEMENT

This study was supported by Scientific research grant of the Ministry of Education, Science and Culture of Japan.

REFERENCES

1) Schenck JF, Jolesz FA, Roemer PB, et al. : Superconducting open-configuration MR imaging system for image-guided therapy. Radiology 1995 ; 195 : 805–814
2) Duckwiler G, Lufkin RB, Teresi L, Spickler E, Dion J, Vinuela F, Bentson J, Hanafee W : Head and neck lesions : MR-guided aspiration biopsy. Radiology 1989 ; 170 : 519–522
3) Levy RM, Breit R, Russell E, Dal Canto MC : MR-guided stereotaxic brain biopsy in neurologically symptomatic AIDS patients. J Acquir Immune Defic Syndr 1991 ; 4(3) : 254–260
4) Pitt AM, Fleckenstein JL, Greenlee RG Jr, Burns DK, Bryan WW, Haller R : MRI-guided biopsy in inflammatory myopathy : initial results. Magn Reson Imaging 1993 ; 11(8) : 1093–1099
5) Mahfouz AE, Rahmouni A, Zylbersztejn C, Mathieu D : MR-guided biopsy using ultrafast T_1- and T_2-weighted reordered turbo fast low-angle shot sequences : feasibility and preliminary clinical applications. AJR 1996 ; 167 : 167–169
6) Buecker A, Adam G, Neuerburg J, Glowinski A, van Vaals JJ, Guenther RW : First clinical results with a single-shot zoom-imaging sequence "local look" for high-resolution subsecond interventional MR procedures. Proceedings. ISMRM 1996 ; 779
7) Ortendahl DA, Kaufman L : Real-time interactions in MRI. Comput Biol Med 1995 ; 25(2) : 293–300
8) Lewin JS, Duerk JL, Jain VR, Petersilge CA, Chao CP, Haaga JR : Needle localization in MR-guided biopsy and aspiration : effects of field strength, sequence design, and magnetic field orientation. AJR 1996 ; 166 : 1337–1345
9) Faber SC, Stehling MK, Reiser M : Artifacts of MR-compatible biopsy needles : optimization of pulse sequences, dependence on MR-parameters, comparison of different products. Proceedings. ISMRM 1996 ; 1741
10) Sinha S, Sinha U, Lufkin R, Hanafee W : Pulse sequence optimization for use with a biopsy needle in MRI. Magn Reson Imaging 1989 ; 7 : 575–579
11) Lufkin R, Teresi L, Chiu L, Hanafee W : A technique for MR-guided needle placement. AJR 1988 ; 151 : 193–196